Liquid Crystals
Publication details, including instructions for authors and subscription information:
http://www.informaworld.com/smpp/title~content=t713926090

Conoscopic study of the $S_{c\alpha}$* phase and the Devil's staircase in an antiferroelectric liquid crystal

Tadaaki Isozaki[a]; Kazuyuki Hiraoka[a]; Yoichi Takanishi[a]; Hideo Takezoe[a]; Atsuo Fukuda[a]; Yoshiichi Suzuki[b]; Ichiro Kawamura[b]
[a] Department of Organic and Polymeric Materials, Tokyo Institute of Technology, Tokyo, Japan [b] Central Research and Development Laboratory, Showa Shell Sekiyu K.K., Kanagawa, Japan

To cite this Article Isozaki, Tadaaki , Hiraoka, Kazuyuki , Takanishi, Yoichi , Takezoe, Hideo , Fukuda, Atsuo , Suzuki, Yoshiichi and Kawamura, Ichiro(1992) 'Conoscopic study of the $S_{c\alpha}$* phase and the Devil's staircase in an antiferroelectric liquid crystal', Liquid Crystals, 12: 1, 59 — 70
To link to this Article: DOI: 10.1080/02678299208029038
URL: http://dx.doi.org/10.1080/02678299208029038

LIQUID CRYSTALS, 1992, VOL. 12, No. 1, 59–70

Conoscopic study of the $S^*_{C_\alpha}$ phase and the Devil's staircase in an antiferroelectric liquid crystal

by TADAAKI ISOZAKI†‡, KAZUYUKI HIRAOKA‡, YOICHI TAKANISHI‡, HIDEO TAKEZOE*‡, ATSUO FUKUDA‡, YOSHIICHI SUZUKI§ and ICHIRO KAWAMURA§

‡Tokyo Institute of Technology, Department of Organic and Polymeric Materials, O-okayama, Meguro-ku, Tokyo 152, Japan

§Showa Shell Sekiyu K.K., Central Research and Development Laboratory, 123-1 Shimokawairi, Atsugi, Kanagawa 243-02, Japan

(*Received 17 September 1991; accepted 26 November 1991*)

The molecular orientational structure of the $S^*_{C_\alpha}$ phase has been studied by means of X-ray, dielectric and conoscopic measurements for 4-(1-methylheptyloxycarbonyl)phenyl 4′-octylcarbonyloxybiphenyl-4-carboxylate. It was found by X-ray scattering that the $S^*_{C_\alpha}$ phase is tilted. According to the conoscopic observation under a low field, the optic plane of $S^*_{C_\alpha}$ is parallel to the field direction similar to that of the $S^*_{C_\gamma}$ phase of 4-(1-methylheptyloxycarbonyl)phenyl 4′-octyloxybiphenyl-4-carboxylate. It was also found that the molecular orientation of the $S^*_{C_\alpha}$ phase is antiferroelectric in the high temperature region, while in the low temperature region it is ferrielectric and changes with temperature, suggesting the so-called Devil's staircase. The critical temperature, where the biaxiality and the tilt angle of the average optic axis have maximum values, was assigned to the ferrielectric state with the largest spontaneous polarization.

1. Introduction

In previous papers, Takanishi *et al.* [1] and Hiraoka *et al.* [2] concluded that competition between the two kinds of molecular interactions gives rise to the $S^*_{C_\alpha}$ phase [3–5] which was discovered between the S_A and S^*_C phases in 4-(1-methylheptyloxycarbonyl)phenyl 4′-octyloxybiphenyl-4-carboxylate (MHPOBC),

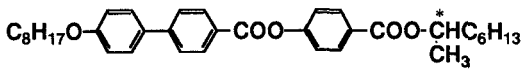

One is the interaction that causes tilting of the molecules from the layer normal in the same direction and sense throughout the smectic layers and hence stabilizes the ordinary S_C phase; the other is the interaction between the spontaneous polarizations that favours tilting of the molecules in the same direction but in the opposite senses in the neighbouring smectic layers. As a result of delicate balancing of these two interactions, a variety of molecular orientational structures appear one after another in the $S^*_{C_\alpha}$ phase. Such a successive structural change was regarded as the Devil's staircase [1, 2, 6, 7].

* Author for correspondence.
† On leave from Showa Shell Sekiyu K.K., Central Research & Development Laboratory.

0267-8292/92 $3·00

Typically, two types of the Devil's staircase are conceivable; one is produced by the temperature change and the other by the applied electric field. The electric field induced Devil's staircase was rather clearly observed in the electric field induced tilt angle [2]. Owing to a lack of proper methods to clarify the molecular orientational structure without causing any perturbation by the application of an external field, the temperature induced Devil's staircase was, however, confirmed to exist only indirectly by carefully analysing the switching current and optical response behaviour [1]. In MHPOBC, a very narrow temperature range of $S^*_{C_\alpha}$ phase (not more than 1°C) was another obstacle to the observation of the temperature induced Devil's staircase. The purpose of this paper is to explore the possibilities of elucidating the molecular orientational structure at zero field by observing the electric field dependence of conoscopic figures.

2. Experimental procedures

The sample used was an antiferroelectric liquid crystal, 4-(1-methylheptyloxycarbonyl)phenyl 4′-octylcarbonyloxybiphenyl-4-carboxylate (MHPOCBC)

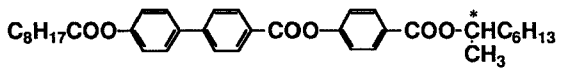

with the following phase sequence on cooling given by DSC [8];

$$\text{I}\ 147°\text{C}\ \text{S}_\text{A}\ 105{\cdot}5°\text{C}\ \text{S}^*_{\text{C}_\alpha}\ 99{\cdot}5°\text{C}\ \text{S}^*_{\text{C}_\text{A}}\ 73{\cdot}3°\text{C}\ \text{S}^*_{\text{I}_\text{A}}\ 66{\cdot}1°\text{C}$$

The identification of the $S^*_{C_\alpha}$ phase was made by miscibility studies with MHPOBC. Note that the present material MHPOCBC has a much wider temperature range for the $S^*_{C_\alpha}$ phase ($\sim 6°$C) than that of MHPOBC ($\sim 1°$C).

For X-ray and dielectric measurements, we prepared homogeneously aligned cells; about 150 μm thick substrate glass plates with ITO were coated with polyimide (Toray, SP-550) and one of them was rubbed unidirectionally. The sample thickness was 24·4 μm. The X-ray scattering measurements with Rigaku RU-200 (Cu–K_α) and the dielectric measurements using an impedance analyser (Hewlett–Packard, LF4192A) were performed by applying 0·1 V_{pp} as previously described [1].

For conoscopic observations [9], we made homeotropically aligned cells using substrate glass plates treated with a surfactant (Toray Dow Corning Silicone, AY-43-021). Two pieces of polyethylene terephthalate (PET) film covered with sheets of aluminium foil were used as spacers and electrodes. The cell thickness was 228 μm and the electrode gap for applying an electric field was 1·7 mm. Conoscopic figures were observed as described previously [9]. A He–Ne laser beam was expanded to a diameter of 4 mm and focused on to the middle of the cell using an objective lens (Nikon FM Plan ELWD) of high magnification ($\times 40$) with ultralong working distance (10 mm) and large numerical aperture (0·5). The temperature controlled oven containing the cell was located between crossed polarizers. Conoscopic figures were displayed on a screen about 93 mm apart from the cell and were photographed. An electric field was applied parallel to the smectic layer along the 45° direction with respect to the polarizer axes. In order to apply a high field, an operational power supply (Hamamatsu, Regulated DC supply Model C665) was used.

3. Experimental results

3.1. *X-ray and dielectric measurements*

It was already concluded for MHPOBC that the $S^*_{C_\alpha}$ phase is a tilted phase [1]. Since the $S^*_{C_\alpha}$ phase temperature range for MHPOBC is very narrow, we repeated the same measurements for MHPOCBC. The $S^*_{C_\alpha}$ phase temperature range as wide as about 6°C will provide a further sound basis to that conclusion. Figure 1 (*a*) shows the temperature dependence of the layer tilt angle and the dielectric constant at 10 kHz obtained for a heating process. The transition temperature between the S_A and $S^*_{C_\alpha}$ phases is identified by the dielectric constant peak which reflects a soft mode contribution in the S_A phase [8, 10]. The transition to the $S^*_{C_A}$ phase is recognized as a decrease in the dielectric constant at low temperatures [8, 10]. These three phases are also identified by texture observations. Since the transition temperatures are influenced by cell thickness, they are slightly different from the ones obtained by DSC. The difference may partially result from a slight inaccuracy in measuring the temperature. In the $S^*_{C_A}$ phase, the layer tilt angle is about 8° and scarcely depends on the temperature. After the $S^*_{C_A}$–$S^*_{C_\alpha}$ phase transition, the chevron angle starts to decrease rather steeply with increasing temperature. Even in the S_A phase, there exists a chevron structure [11] but the angle keeps a small constant value just after the phase transition.

A similar temperature dependence was observed in the layer tilt angle for a cooling process as shown in figure 1 (*b*); the chevron angle starts to increase with decreasing temperature after the S_A–$S^*_{C_\alpha}$ phase transition. The dielectric constant, however, shows a slightly different behaviour; the dielectric constant for the cooling process is larger than that for the heating process in the low temperature region of the $S^*_{C_\alpha}$ phase. We can also find such a result in the incommensurate (IC) phase transition of some dielectric materials [12]. These results suggest that the $S^*_{C_\alpha}$ phase is a tilted phase and the tilt angle depends on the temperature.

Both for the heating and cooling processes, the S_A–$S^*_{C_\alpha}$ transition temperature, determined from the dielectric constant peak, is slightly higher than that corresponding

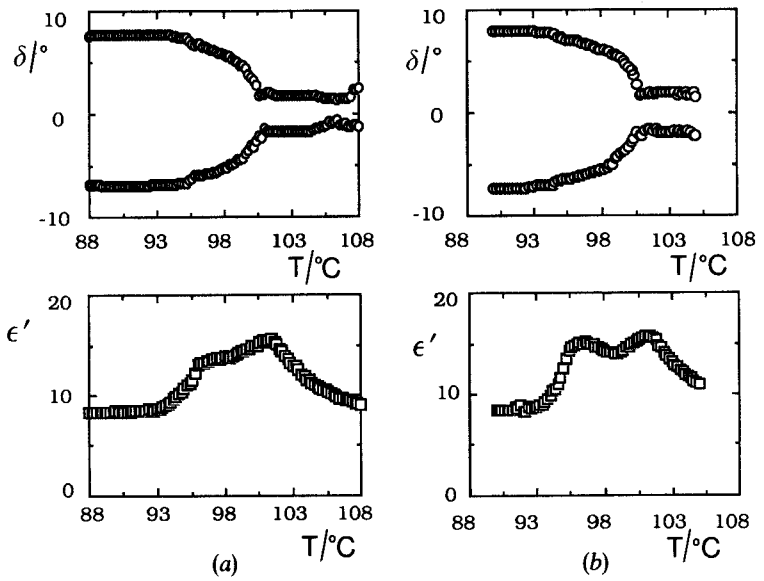

Figure 1. The temperature dependence of layer tilt angle δ and dielectric constant ϵ' at 10 kHz; (*a*) for a heating process and (*b*) for a cooling process.

to the beginning of a steep change in the layer tilt angle. According to the *T–E* diagram for MHPOBC [13], we cannot imagine that an electric field of 0·1 V_{pp} applied for the dielectric measurements influences the transition temperature. The reason for the different transition temperatures in the two measurements is not known at present.

3.2. *Conoscopic measurements*

Figure 2 shows two series of photographs of the conoscopic figures under several field strengths taken in (*a*) the $S^*_{C_A}$ and (*b*) the $S^*_{C_\alpha}$ phases. Since the cell was different from the one used for the X-ray and dielectric constant measurements, the phase transition temperatures are different from those shown in figure 1. The S_A–$S^*_{C_\alpha}$ transition temperature is about 106°C, which is determined from the maximum of the electroclinic effect, whereas the $S^*_{C_\alpha}$–$S^*_{C_A}$ transition temperature is about 100°C, and is found from the optic plane change. In the $S^*_{C_A}$ phase, the conoscopic figures are similar to those previously reported by Gorecka *et al.* [9]; the biaxiality appears but centre shift is scarcely observed because the dielectric anisotropy is responsible for their changes. The very slight centre shift may originate from the pretransitional effect [14]. Figure 3 summarizes the electric field dependence of $n_{mid} - n_{min}$ in the $S^*_{C_A}$ phase.

In the $S^*_{C_\alpha}$ phase, a complicated field dependence was observed. The centre shifts toward the same direction as for the S^*_C and $S^*_{C_\gamma}$ phases of MHPOBC [9], but the amount is much smaller. The optic plane is parallel to the field direction as in the $S^*_{C_\gamma}$ phase of MHPOBC. The biaxiality under similar, low field strengths is, however, much smaller than that in the $S^*_{C_\gamma}$ phase of MHPOBC. The detailed measurements with fine field increments show that the biaxiality, n_{mid}–n_{min}, changes drastically at around 176 V mm^{-1} as illustrated in figure 4. Figure 5 shows the electric field dependence of the tilt angle of the average optic axis, θ_{tilt}, in the $S^*_{C_\alpha}$ phase, which also indicates a two step change at least below 102·5°C with the inflection point at about 176 V mm^{-1}.

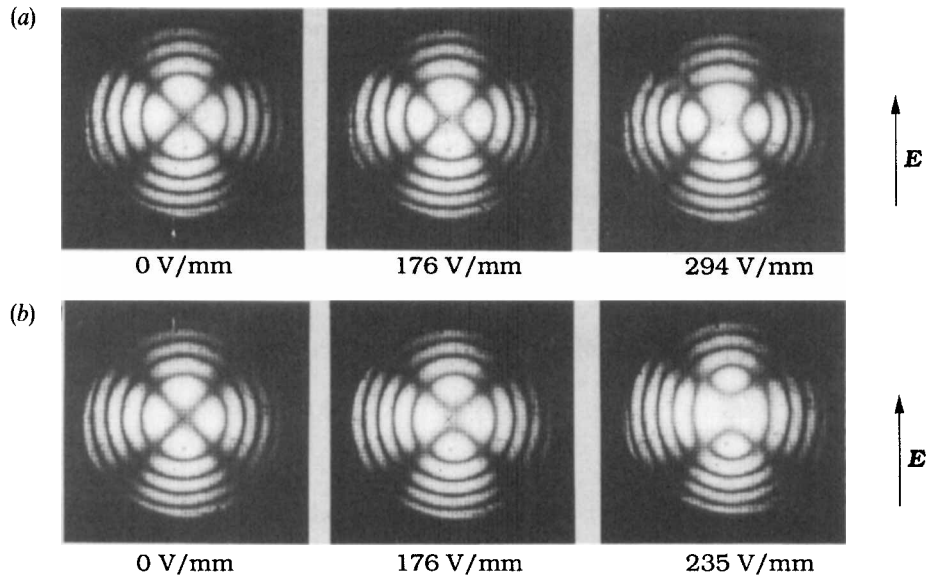

Figure 2. Two series of conoscopic figures under several field strengths; (*a*) in the $S^*_{C_A}$ phase and (*b*) in the $S^*_{C_\alpha}$ phase.

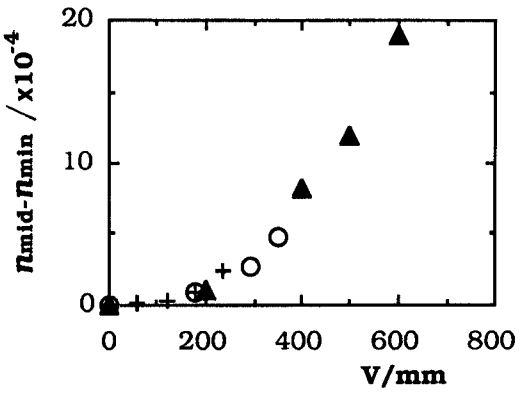

Figure 3. The electric field dependence of n_{mid}–n_{min} in the $S^*_{C_A}$ phase. ○, $T-T_C=-1{\cdot}9°C$; ▲, $T-T_C=-0{\cdot}7°C$; +, $T-T_C=-0{\cdot}2°C$.

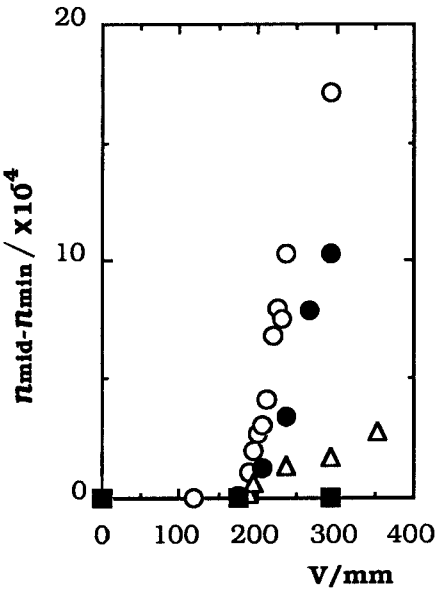

Figure 4. The electric field dependence of n_{mid}–n_{min} in the $S^*_{C_\alpha}$ phase. n_{mid}–n_{min} starts to appear at around 176 V mm^{-1}. ○, 102·2°C; ●, 102·5°C; △, 104·0°C; ■, 105·0°C.

Conoscopic figures for a field strength of 176 V mm^{-1} at various temperatures for the cooling process are shown in figure 6. The biaxiality is largest at about 102·8°C and becomes smaller with either increasing or decreasing temperature. This temperature behaviour of the biaxiality is quantitatively summarized in figure 7, where n_{mid}–n_{min} under 167 V mm^{-1} and 389 V mm^{-1} is given as a function of temperature. It is obvious that the $S^*_{C_\alpha}$ phase can be divided into two temperature regions separated by a critical temperature, ~103°C. We also recall the different behaviour above and below the critical temperature observed for the dielectric measurement shown in figure 1; the difference in the heating and cooling runs exists below the critical temperature but not above it. The biaxiality attains its largest value at the critical temperature when the

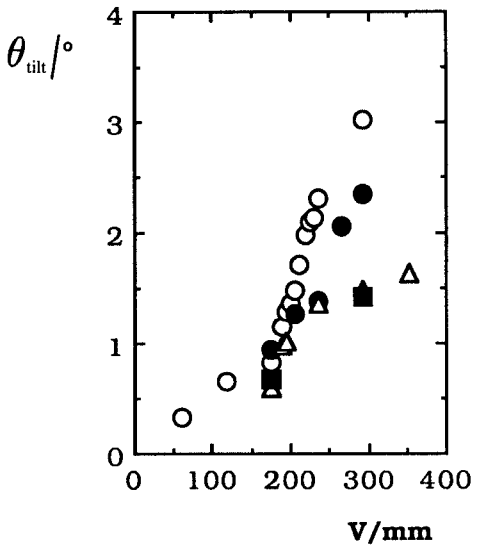

Figure 5. The electric field dependence of θ_{tilt} in the $S^*_{C_\alpha}$ phase. Note that a two step change is observed with the inflection point at about 176 V mm^{-1}. ○, 102·2°C; ●, 102·5°C; △, 104·0°C; ■, 105·0°C.

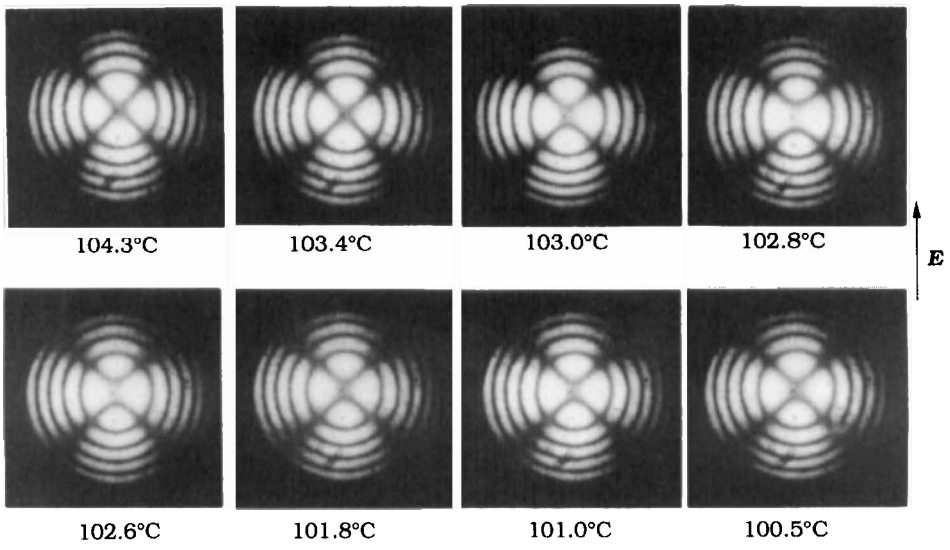

Figure 6. Conoscopic figures for $S^*_{C_\alpha}$ phase under 176 V mm^{-1} at various temperatures for the cooling process. The biaxiality is largest at 102·8°C.

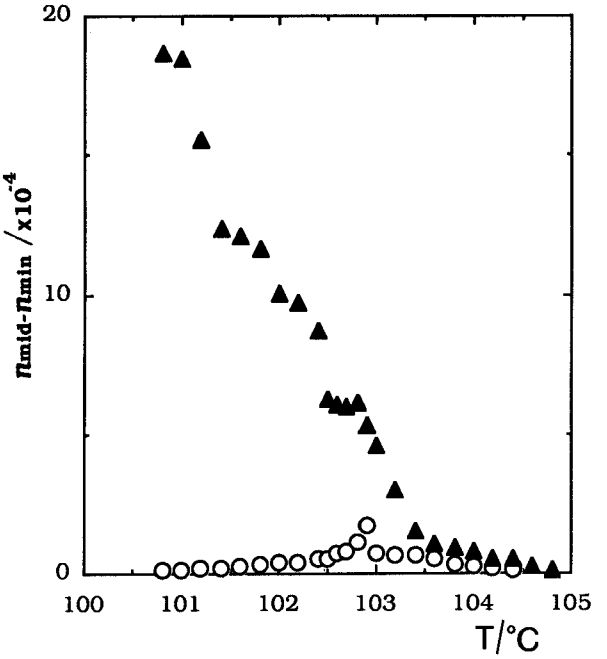

Figure 7. The temperature dependence of $n_{mid}-n_{min}$ for the $S^*_{C_\alpha}$ phase observed under 167 V mm^{-1} and 389 V mm^{-1}. The biaxiality attains its largest value at the critical temperature around 103°C under 167 V mm^{-1}, while it increases with decreasing temperature under 389 V mm^{-1}. ○, 167 V mm^{-1}; ▲, 389 V mm^{-1}.

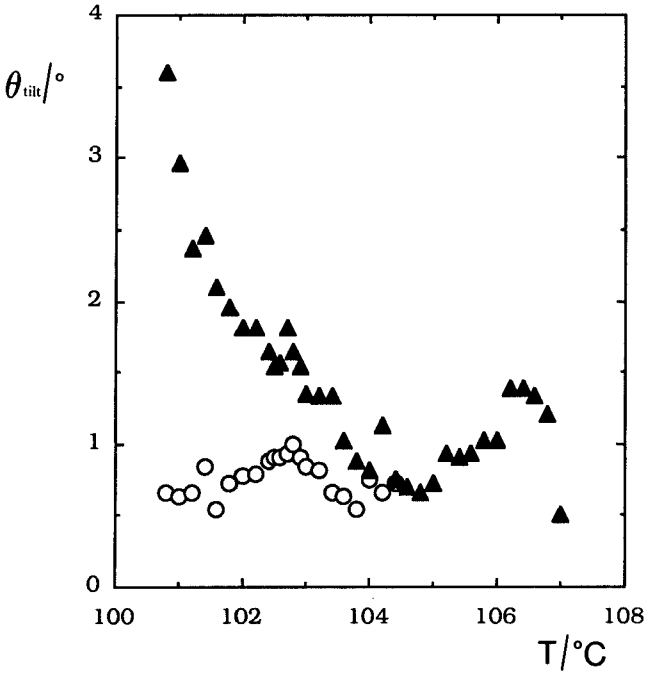

Figure 8. The temperature dependence of θ_{tilt} for the $S^*_{C_\alpha}$ phase observed under 167 V mm^{-1} and 389 V mm^{-1}. The peak at about 106°C is due to the S_A to $S^*_{C_\alpha}$ transition and the maximum at about 103°C is in a good agreement with the critical temperature in figure 7. ○, 167 V mm^{-1}; ▲, 389 V mm^{-1}.

applied field is below 176 V mm^{-1}. It was also confirmed, as illustrated in figure 8, that θ_{tilt} obtained from conoscopic observations gives rise to a peak at the critical temperature. Below the critical temperature, the difference in the values of n_{mid}–n_{min} and θ_{tilt} under 167 V mm^{-1} and 389 V mm^{-1} is remarkable. This observation suggests the existence of a field strength which brings about an abrupt structural change in this temperature range.

4. Discussion

Let us first explain qualitatively the basis of the above experimental results that the $S^*_{C_\alpha}$ phase of MHPOCBC is also the Devil's staircase. In the low temperature region, since the optic plane is the same as that in the $S^*_{C_\gamma}$ phase, the structure of the $S^*_{C_\alpha}$ phase is expected to be similar to that of the ferrielectric $S^*_{C_\gamma}$ phase. In the high temperature region, the biaxiality, n_{mid}–n_{min}, does not appear under a low field. This behaviour is found to be characteristic of antiferroelectricity; neither the spontaneous polarization nor the small dielectric anisotropy, due to the small tilt angle, cause the helix unwinding.

At the critical temperature, n_{mid}–n_{min} becomes a maximum. The biaxiality should become large as the helix unwinding proceeds and/or the tilt angle becomes large. The tilt angle increases with decreasing temperature as indicated by the temperature dependence of the layer tilt angle as shown in figure 1. Therefore, the large n_{mid}–n_{min} value at about 103°C implies the higher degree of helix unwinding is caused by the large spontaneous polarization. Thus, at the critical temperature, the ferrielectric molecular orientation with the largest spontaneous polarization is realized. The fact that both n_{mid}–n_{min} and θ_{tilt} become smaller with decreasing temperature strongly suggests the decreasing spontaneous polarization leads to the successive orientational and structural changes, namely the emergence of the Devil's staircase.

Let us next examine the extent to which the one dimensional Ising model used in [1] describes the above experimental results. By assigning the spin-down state to the antiferroelectic ordering of the neighbouring smectic layers and the spin-up state to the ferroelectric ordering, any molecular orientational structure expected to appear is specified by an irreducible fraction q_T of the ferroelectric ordering in the antiferroelectic ordering. The irreducible fraction numbers q_Ts and the corresponding spontaneous polarizations constitute as a whole the Farey sequence (see figure 9). Every rational number with the denominator smaller than 13 is shown with increasing denominator from line to line. The molecular structures with $q_T = m/7$ ($m = 1, 2, \ldots, 6$) are, for example given in figure 10(*a*), where * indicates those structures with ferroelectric ordering; the remaining structures possess antiferroelectric ordering. The position Z_i of the ith ferroelectric ordering is given by the simple formula; $Z_i = \text{integer}(i/q_T)$. As is clear in these examples, the structures with $q_T = m/n$ represent antiferroelectric structures when either m or n is even; otherwise it represents a ferrielectric structure with spontaneous polarization $P_s(\text{ferro})/n$, where $P_s(\text{ferro})$ is the expected spontaneous polarization of the corresponding ferroelectric structure with the same tilt angle. In the Farey sequence, those q_Ts representing a ferrielectric structure are shown as bold and italic letters. For $n = 7$, for instance, the structures with $q_T = 1/7$, 3/7 and 5/7 are ferrielectric as shown in figure 10(*a*). Note, in particular, that the structure with $q_T = 1/2$ is antiferroelectric; the ferrielectric structure with $q_T = 1/3$ has the maximum proportion of $P_s(\text{ferro})$ and is exactly the same as that of $S^*_{C_\gamma}$ [15].

The structure with $q_T = 0$ appears immediately after the S_A to $S^*_{C_\alpha}$ transition. As the temperature decreases, structures with larger q_Ts emerge one after another. It was

actually observed in switching current measurements under a triangular wave that the number of peaks changes with temperature in a very complicated way; the even and odd numbers of peaks represent the antiferroelectric and the ferrielectric structures in the absence of an electric field, respectively. The stability of each structure cannot as yet be predicted, because the long range repulsive interaction in the one dimensional Ising model has not yet been characterized.

When the applied electric field is weak, for example lower than a critical field ($\sim 176\ \mathrm{V\,mm^{-1}}$), the induced biaxiality, $n_{\mathrm{mid}}-n_{\mathrm{min}}$, and the induced tilt angle, θ_{tilt}, must result from the helix unwinding [9]. The longer the helical pitch is and the larger the spontaneous polarization is, the easier the unwinding occurs. Although no direct observation of the helical pitch has yet been made, it is reasonable to assign the peaks at the critical temperature, $\sim 103°C$, in figures 7 and 8 to the structure with $q_T = 1/3$ which has the maximum proportion of P_s(ferro). The reason why neither the induced biaxiality nor the induced tilt angle show any stepwise change suggesting the temperature induced Devil's staircase may at least partly be due to the inaccuracy of our measurements.

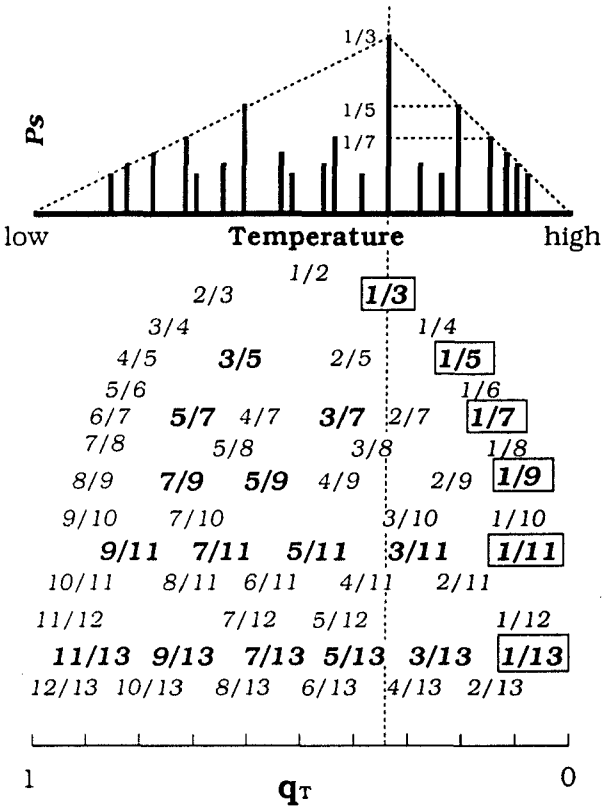

Figure 9. The irreducible fraction numbers q_Ts constitute as a whole the Farey sequence. The numbers representing the ferrielectric structures are shown as bold and italic letters and those representing antiferroelectric structures are shown as ordinary italic letters. Note that the ferrielectric structures realizing not only the temperature induced but also the field induced Devil's staircase are indicated by the numbers enclosed by rectangles. The corresponding spontaneous polarizations P_ss are indicated by bars at q_Ts on the abscissa of unit length.

As mentioned in the Introduction, there is a field induced Devil's staircase in addition to the temperature induced Devil's staircase. The structure in the field induced Devil's staircase is specified by an irreducible fraction q_E of the tilting sense opposite to that stabilized under a sufficient field strength. Note that the structures with $q_T = 1/(2l+1)$ in the temperature induced Devil's staircase, as indicated by enclosed rectangles in figure 9, are exactly the same as those with $q_E = l/(2l+1)$ in the field induced Devil's staircase [2] as illustrated in figures 10 (*a*) and (*b*), where $l = 1, 2, 3, \ldots$. As the applied electric field becomes stronger than the critical field ($\sim 176\ \mathrm{V\ mm^{-1}}$), it must cause a structural change due to a changeover from a temperature induced staircase to a field induced staircase. In the temperature region higher than the critical temperature ($\sim 103°\mathrm{C}$), the change may occur rather smoothly, because the dense arrangement of structures with $q_T = 1/(2l+1)$ are equivalent to those with $q_E = l/(2l+1)$.

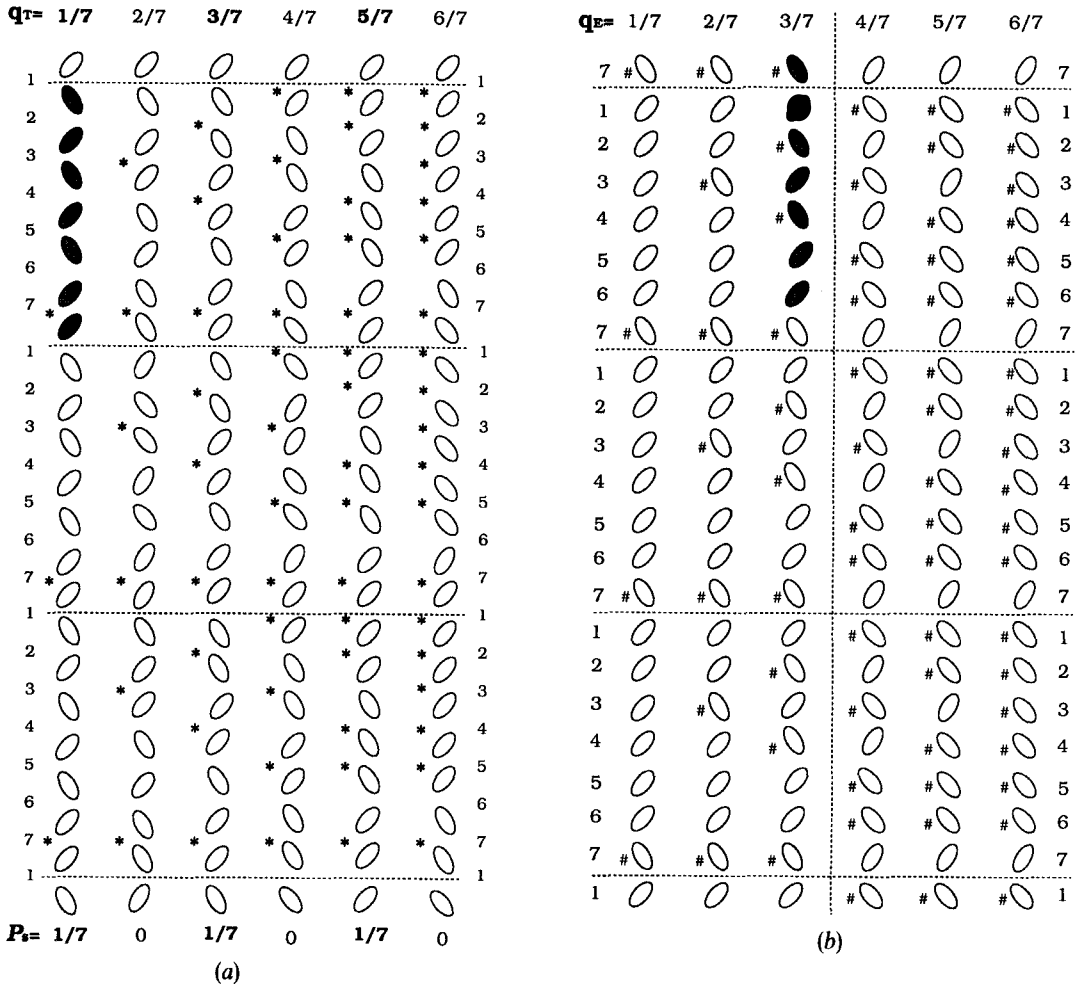

Figure 10. The structures with (*a*) $q_T = m/7$ ($m = 1, 2, \ldots, 6$) for the temperature induced Devil's staircase and (*b*) $q_E = m/7$ ($m = 1, 2, \ldots, 6$) for the field induced Devil's staircase. Note that the hatched structures for $q_T = 1/7$ and $q_E = 3/7$ are identical. With increasing q, the ferroelectric ordering and the oppositely tilted molecules indicated by * and # increase in (*a*) and (*b*), respectively.

In the temperature region lower than the critical temperature ($\sim 103°C$), an abrupt changeover from a temperature induced staircase to a field induced staircase occurs, since there exist no $q_T = 1/(2l+1)$ in this temperature region. The large biaxiality and tilt angle under a high field of 389 V mm^{-1} in the low temperature region in figures 7 and 8 must be due to this changeover. These structural changes were also observed in the plot of induced tilt angle versus field strength for MHPOBC [2].

In this way, an attempt to understand the electric field dependence of conoscopic figures in the $S^*_{C_\alpha}$ phase temperature range leads to the understanding of the $S^*_{C_\alpha}$ phase structure at zero field; the existence of the critical temperature is, at least qualitatively, successfully ascribed to the appearance of the structure with $q_T = 1/3$ which has the maximum proportion of P_s(ferro), P_s(ferro)/3. An objection to this attempt may be raised because the $S^*_{C_\alpha}$ phase in MHPOCBC is followed not by a ferroelectric S^*_C phase but by an antiferroelectric $S^*_{C_A}$ phase and hence an increase in the ferroelectric ordering with decreasing temperature, i.e. the fundamental assumption made in [1] and [2] may not be correct. However, the mere non-existence of the ferroelectric S^*_C phase on the low temperature side does not always deny the increase in the ferroelectric ordering, particularly when the $S^*_{C_\alpha}$ to $S^*_{C_A}$ transition is of first order [8]. To arrive at a conclusion on a reasonable basis, we have tried to improve the method of observing conoscopic figures using a CCD camera as well as the image processing technique. It is also helpful to find a compound that has a wide $S^*_{C_\alpha}$ phase temperature range followed directly by an S^*_C phase.

5. Conclusions

After showing that the $S^*_{C_\alpha}$ phase in MHPOCBC is a tilted phase by means of X-ray measurements, the molecular orientational structure of the $S^*_{C_\alpha}$ phase was investigated by conoscopic observation under an electric field. The biaxiality and the tilt angle of the average optic axis have maximum values at a mid-temperature range of this phase, where a ferrielectric state, $q_T = 1/3$, with the maximum spontaneous polarization P_s(ferro)/3 appears. Above and below this temperature, various ferrielectric and antiferroelectric states successively appear. The results were explained by the emergence of the Devil's staircase. The behaviour of the changeover between a temperature induced staircase and a field induced staircase was also discussed above and below the critical temperature separately; i.e. smooth and abrupt changeovers in the respective temperature ranges depend on whether or not the equivalent structure exists in both the temperature induced and the field induced staircases.

This work was partly supported by a Grant in Aid for Scientific Research (#03205045) from the Ministry of Education, Science and Culture.

References

[1] Takanishi, Y., Hiraoka, K., Agrawal, V. K., Takezoe, H., Fukuda, A., and Matsushita, M., 1991, *Jap. J. appl. Phys.*, **30**, 2023.

[2] Hiraoka, K., Takanishi, Y., Skarp, K., Takezoe, H., and Fukuda, A., 1991, *Jap. J. appl. Phys.*, **30**, L1819.

[3] Fukui, M., Orihara, H., Yamada, Y., Yamamoto, N., and Ishibashi, Y., 1989, *Jap. J. appl. Phys.*, **28**, L849.

[4] Chandani, A. D. L., Ouchi, Y., Takezoe, H., Fukuda, A., Terashima, K., Furukawa, K., and Kishi, A., 1989, *Jap. J. appl. Phys.*, **28**, L1261.

[5] Takezoe, H., Lee, J., Chandani, A. D. L., Gorecka, E., Ouchi, Y., and Fukuda, A., 1991, *Ferroelectrics*, **114**, 187.

[6] BAK, P., 1986, *Physics Today*, **39** (12), 38.
[7] BAK, P., 1982, *Phys. Rev. Lett.*, **49**, 249.
[8] ISOZAKI, T., SUZUKI, Y., KAWAMURA, I., MORI, K., YAMAMOTO, N., YAMADA, Y., ORIHARA, H., and ISHIBASHI, Y., 1991, *Jap. J. appl. Phys.*, **30**, L1573.
[9] GORECKA, E., CHANDANI, A. D. L., OUCHI, Y., TAKEZOE, H., and FUKUDA, A., 1990, *Jap. J. appl. Phys.*, **29**, 131.
[10] HIRAOKA, K., TAGUCHI, A., OUCHI, Y., TAKEZOE, H., and FUKUDA, A., 1990, *Jap. J. appl. Phys.*, **29**, L103.
[11] OUCHI, Y., TAKANISHI, Y., TAKEZOE, H., and FUKUDA, A., 1989, *Jap. J. appl. Phys.*, **28**, 2547.
[12] UNRUH, H. G., 1984, *Ferroelectrics*, **53**, 319.
[13] HIRAOKA, K., CHANDANI, A. D. L., GORECKA, E., OUCHI, Y., TAKEZOE, H., and FUKUDA, A., 1990, *Jap. J. appl. Phys.*, **29**, L1473.
[14] JOHNO, M., ITOH, K., LEE, J., OUCHI, Y., TAKEZOE, H., and FUKUDA, A., 1990, *Jap. J. appl. Phys.*, **29**, L107.
[15] TAKEZOE, H., LEE, J., OUCHI, Y., and FUKUDA, A., 1991, *Molec. Crystals liq. Crystals*, **202**, 85.